Preprint Cambridge Centre for Computational Chemical Engineering ISSN 1473 – 4273

HCCI Combustion Control Using Dual-Fuel Approach: Experimental and Modeling Investigations

Ali Aldawood [1], Sebastian Mosbach [1], Markus Kraft [1]

released: 16 January 2012

[1] Department of Chemical Engineering
and Biotechnology
University of Cambridge
New Museums Site
Pembroke Street
Cambridge, CB2 3RA
United Kingdom
E-mail: mk306@cam.ac.uk

Preprint No. 114

Keywords: HCCI control, dual-fuel HCCI, multiobjective optimization, stochastic reactor model

Edited by
Computational Modelling Group
Department of Chemical Engineering and Biotechnology
University of Cambridge
New Museums Site
Pembroke Street
Cambridge CB2 3RA
United Kingdom

Fax: + 44 (0)1223 334796
E-Mail: c4e@cam.ac.uk
World Wide Web: http://como.ceb.cam.ac.uk/

Abstract

A dual-fuel approach to control combustion in HCCI engine is investigated in this work. This approach involves controlling the combustion heat release rate by adjusting fuel reactivity according to the conditions inside the cylinder. Experiments were performed on a single-cylinder research engine fueled with different ratios of primary reference fuels and operated at different speed and load conditions, and results from these experiments showed a clear potential for the approach to expand the HCCI engine operation window. Such potential is further demonstrated dynamically using an optimized stochastic reactor model integrated within a MATLAB code that simulates HCCI multi-cycle operation and closed-loop control of fuel ratio. The model, which utilizes a reduced PRF mechanism, was optimized using a multi-objective genetic algorithm and then compared to a wide range of engine data. The optimization objectives, selected based on relevance to this control study, were the cylinder pressure history, pressure rise rate, and gross indicated mean effective pressure (IMEPg). The closed-loop control of fuel ratio employed in this study is based on a search algorithm, where the objective is to maximize the gross work rather than directly controlling the combustion phasing to match preset values. This control strategy proved effective in controlling pressure rise rate and combustion phasing while not needing any prior knowledge or preset information about them. It also ensured that the engine was always delivering maximum work at each operation condition. This is in a sense analogous to the use of maximum brake torque timing in spark-ignition engines. The dynamic model allowed for convenient examination of the dual-fuel approach beyond the limits tested in the experiments, and thus helped in performing an overall assessment of the approach's potential and limitations.

Contents

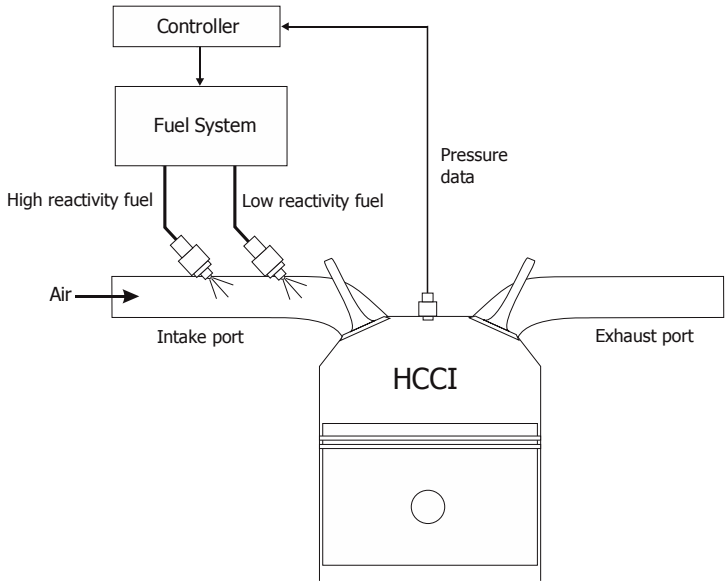

Figure 1: *A schematic of the dual-fuel engine concept. A pressure sensor fitted inside the cylinder provides a pressure feedback signal to a controller, which accordingly decides the best mixing ratio of the two fuels.*

1 Introduction

The Homogeneous-charge compression-ignition (HCCI) concept exhibits attractive emissions and fuel economy characteristics. This makes it a potential alternative to combustion modes currently used in internal combustion engines. Successful application of this concept, however, is still dependent on finding an effective strategy for controlling HCCI combustion over a wide range of operating conditions.

Many HCCI control strategies based on a dual-fuel approach have been suggested and investigated in recent years. Among these is the use of two hydrocarbon fuels with largely different reactivity and combustion characteristics. The combustion in this case is controlled by adjusting fuel reactivity, by the means of mixing of the two fuels, according to the conditions inside the cylinder. Such approach is schematically illustrated in Figure 1. A pressure sensor fitted inside the cylinder provides a pressure feedback signal to a controller, which accordingly decides the best mixing ratio of the two fuels.

Fuels that exhibit multiple stages ignition are known to be more reactive than those exhibiting only a single stage. Characteristics of first-stage ignition also differ among fuels with multiple stages ignition. For instance, n-heptane has a much larger heat release during the first-stage ignition than iso-octane. The larger heat release increases the rate of pressure rise and shortens the delay before the main combustion event (i.e. second-stage ignition) resulting in advanced combustion timing [12, 16].

The above effects exhibited by primary reference fuels (PRF) and many other hydrocarbon fuels could be potentially employed to extend the operating range of the HCCI engine. This potential has been examined in several previous studies. For example, Olsson et al.

[15] investigated a dual-fuel approach that uses primary reference fuels to control HCCI engine, and concluded that such approach was feasible. Similar results were also reported by Atkins and Koch [4] who concluded that varying of fuel octane rating (i.e. the ratio of iso-octane to n-heptane) could be employed to increase the load range of the HCCI engine.

The use of commercial fuels or mixtures of single-component fuels and commercial fuels have been investigated in several more recent studies. Examples of fuels considered include mixtures of ethanol and n-heptane [18]; mixtures of n-heptane and diesel [13]; and mixtures of gasoline and diesel [8, 11]. All of these studies reported some positive results and varying levels of feasibility.

The current paper aims to shed more light on the potential of using primary reference fuels in a dual-fuel strategy to control HCCI combustion. The paper presents new HCCI engine results as well as simulation results that examine wider operating windows, and which are based on a modeling approach that combines reduced chemistry representation with genetic algorithm optimization. The paper also suggests a new way for controlling HCCI combustion based on maximization of obtained work rather than the conventional phasing control.

2 Engine Experiments

The experiments for this work were carried out on a half-liter single-cylinder research engine running in HCCI mode. The specifications of this engine are listed in Table 1. The engine has a pent-roof combustion chamber fitted with four valves. Fuel is delivered intermittently via a port fuel injector located at the end of the intake port just above the intake valves. Intake air passes through a conditioner to adjust its temperature, humidity, and pressure as necessary. All experiments were performed at a boosted intake pressure of 1.5 bar and an intake air temperature of 75^{o}C. The engine was fueled with primary reference fuels at three different volume ratios: PRF40 (i.e. 40% iso-octane and 60% n-heptane), PRF60 and PRF80. Load sweeps were performed at three constant speeds of 1200, 1500 and 1800 rpm. Upper and lower bounds of possible load range are first identified at each test condition, and then test points are selected at reasonably-distanced intervals. The load range is bounded by knocking and misfire limits, identified in this work respectively by a maximum pressure rise rate of 10 bar/deg and a CoV in IMEP of 5%. Experimental data for 300 consecutive cycles are collected at each test point after allowing sufficient operation settling time. The results reported in this section represent average values for the 300 cycles.

The results from these experiments show a clear potential for using the dual-fuel approach to extend the operating range at the three tested speeds. Figure 2 illustrates how gross indicated mean effective pressure (IMEPg) varies with varying equivalence and PRF ratios. Increasing the PRF octane rating extends the upper operation boundary and preserves the engine ability to deliver more work as equivalence ratio increases. The figure also shows the advantage of varying the PRF ratio on the engine positive work at similar operating conditions as well as the critical points when the change must take place to realize such advantage. Gross IMEP, which accounts only for the indicated work during the closed

Table 1: *Engine specifications and valve timing information. Crank angles here are measured relative to firing TDC.*

Parameter	**Value**
Number of cylinders	1
Operation cycle	4-stroke
Combustion mode	HCCI
Number of valves	4
Cylinder displacement (liters)	0.5
Bore x Stroke (mm)	84 x 90
Connecting rod length (mm)	159
Crank radius (mm)	45
Compression ratio	12:1
Fuel delivery system	PFI
Cooling water temperature (^{o}C)	90
Lubrication oil temperature (^{o}C)	90
IVO (CAD)	-356
EVC (CAD)	-352
IVC (CAD)	-156
EVO (CAD)	170

volume, was used here to exclude pumping variations and facilitate comparison with simulation results from the closed-volume model described in the next section.

The boundaries of operation at the tested speeds can be inferred from Figure 3 which shows the readings of maximum pressure rise rate and variation in IMEP. To protect the engine from knocking effects, all test points were selected so that the maximum pressure rise rate didn't exceed 10 bar/deg. The point at the highest equivalence ratio, before reaching the set knocking limit, is chosen to represent the upper boundary of the operation envelope. The lower boundary is determined by a maximum coefficient of variation in IMEP of 5%. The lowest equivalence ratio, before the variation coefficient exceeds 5%, is considered here as the lower boundary of the operation envelope at the respected speed.

Using the conventions described above, the engine operation envelopes for the different PRF ratios are constructed as shown in Figure 4. While the envelopes shrink as the PRF octane rating increases, they also move upward allowing the engine to operate at higher equivalence ratios and to produce more work. These effects generally become more prominent as the speed increases. For example, while changing the PRF octane rating from 40 to 80 at 1200 rpm increases the equivalence range from 0.32 to 0.34 and the IMEPg by about 1 bar, the equivalence ratio increases from 0.31 to 0.38 and the IMEPg increases by about 2 bars at 1800 rpm.

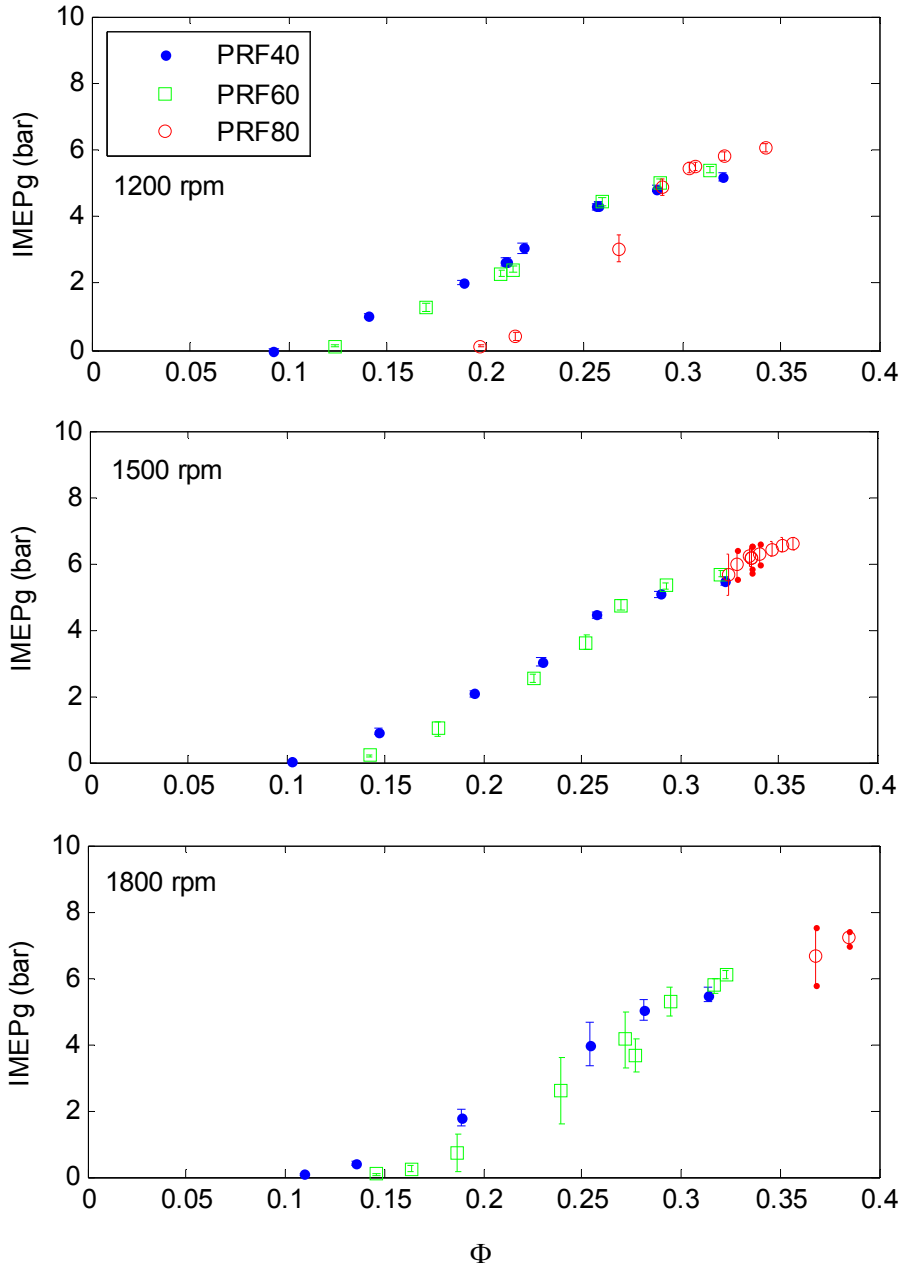

Figure 2: *Gross mean effective pressure for different PRF ratios and operating conditions. Increasing the PRF octane rating extends the upper operation boundary and preserves the engine ability to deliver more work as the equivalence ratio increases. Error bars on experimental data are based on ±1 standard deviation*

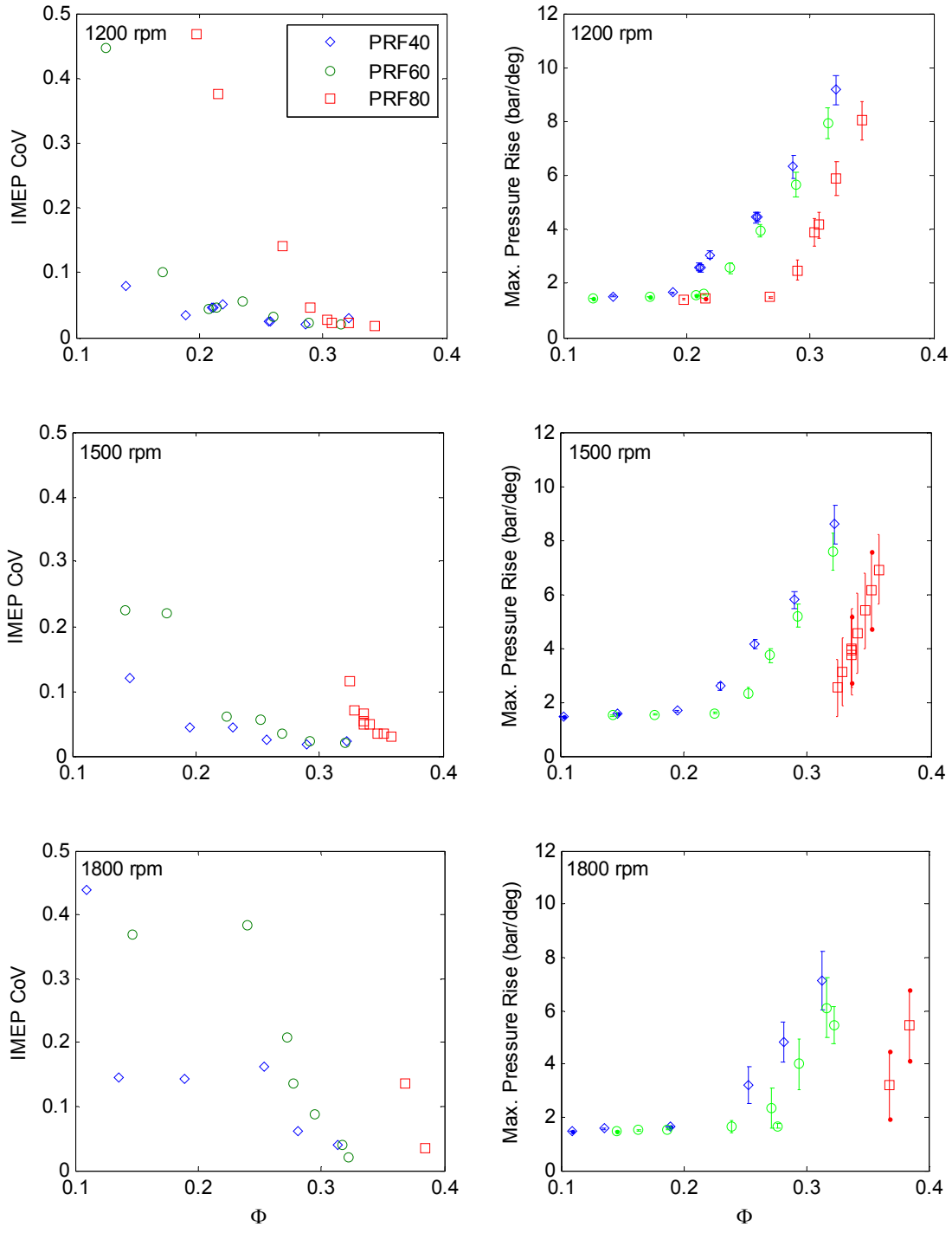

Figure 3: *Maximum pressure rise rate and variation of mean effective pressure for all test points. The point at the highest equivalence ratio, before reaching the set knocking limit of 10 bar/deg, is chosen to represent the upper boundary of the operation envelope. The lower boundary is determined by a maximum coefficient of variation in IMEP of 5%. Error bars on maximum pressure rise values represent ±1 standard deviation.*

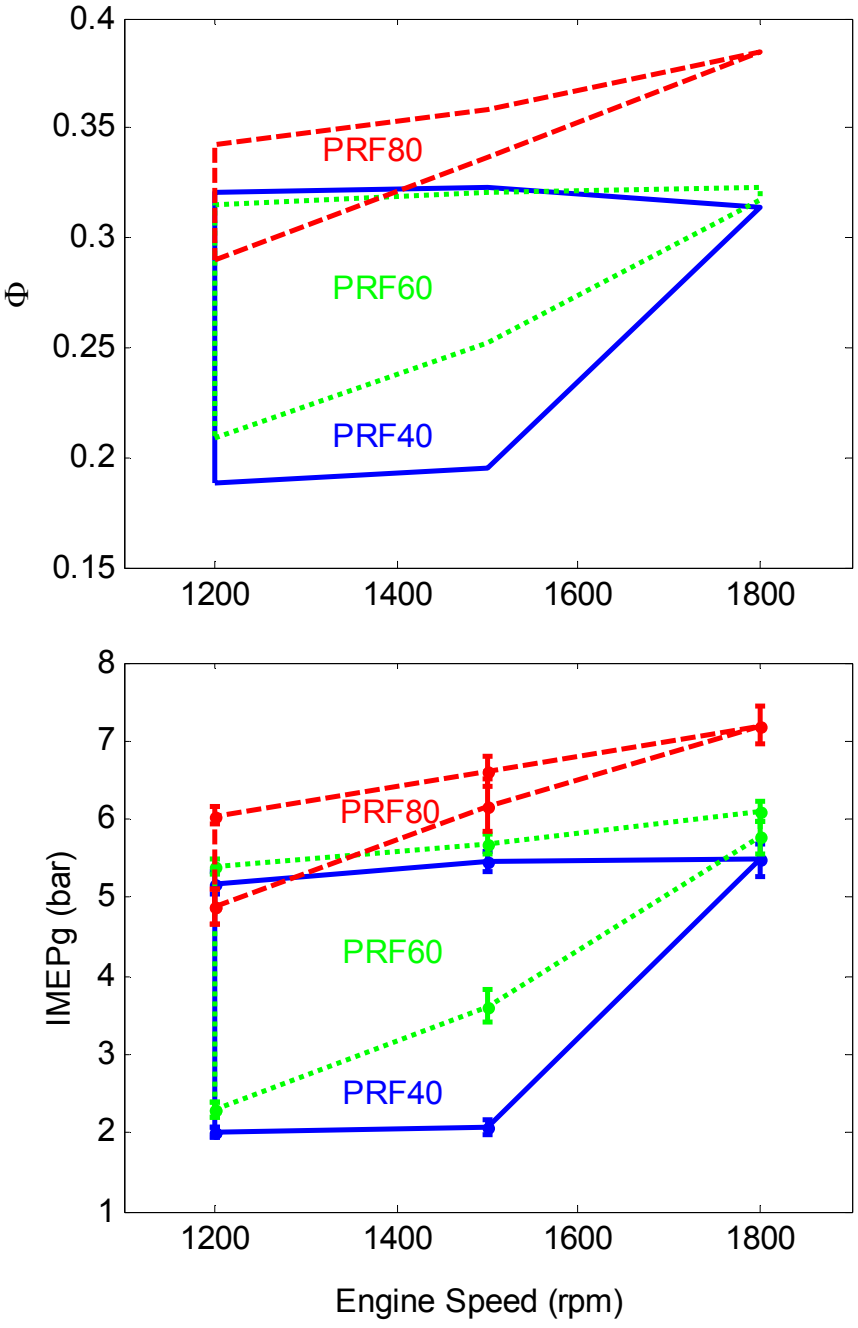

Figure 4: *Engine operation envelopes for different PRF ratios. While the envelopes shrink as the PRF octane rating increases, they also move upward allowing the engine to operate at higher equivalence ratios and to produce more work. These effects generally become more prominent as the speed increases. Error bars on IMEPg values represent ±1 standard deviation.*

3 Model Setup and Optimization

The results from engine experiments showed a clear potential for the dual-fuel approach to expand the HCCI engine operation window. In order to investigate this potential further, a stochastic reactor (SRM) model (see [2, 6, 7, 14]) is used after being optimized for the current engine.

The model uses a fixed residual gas composition extracted from simulation results for an arbitrary but representative operating condition. The ratio of residual gas is determined through the optimization step discussed below. Initial pressures and temperatures at IVC for wide operating ranges, including and extending beyond experimental ranges, were estimated using a GT-Power gas dynamics model developed and calibrated for the current engine. Figure 5 shows the obtained maps of IVC temperature and pressure at 1200 rpm for different PRF octane ratings and equivalence ratios. The maps for different speeds have been integrated within the model to allow simulation of transient operation. These maps indicate that both equivalence ratio and speed had a moderate effect on IVC temperature, but a weak effect on IVC pressure. PRF ratio, on the other hand had little or no effect on IVC pressure and temperature.

The IVC maps incorporate steady-state temperature and pressure values. This prevents the model from considering the thermal inertia effects during transients. To minimize the impact of this on the simulation results, a sufficient settling time will need to be allowed between transient steps. In the current study, a 20-cycle settling time is used in all transient control simulations.

The model utilizes a highly-reduced PRF mechanism that has only 33 species and 38 reactions. Description of this mechanism is given in [17]. The use of this small mechanism was motivated by the need for speedy computations that allow extensive simulation of transient, multi-cycle HCCI engine operation. Two more detailed PRF mechanisms (with 767 and 157 species respectively) were considered initially, and they both performed significantly better than the 33-species mechanism in terms of predicting key engine responses. However, the improved performance of the more detailed mechanisms came with a higher computational time that was deemed not practical for the purpose of this study.

The use of the reduced mechanism along with the other model simplifications (such as using a fixed residual gas ratio and composition) necessitated an optimization step to enhance the model predictivity of engine responses relevant to the current control study. These responses, which constitute the optimization objectives, are the cylinder pressure history, the pressure rise rate, and the gross indicated work (or IMEPg). For this purpose, the model was optimized using a multi-objective genetic algorithm, where the best solutions are searched for using the principles of evolution. Further information about this approach can be found in [3].

The optimization variable set consisted of the three coefficients of Arrhenius equation (i.e. the pre-exponential factor, the temperature exponent and the activation energy) for all reactions, as well as four selected variables from the SRM (average wall temperature, residual gas fraction, turbulent mixing time and heat transfer coefficient). Objective functions for the selected responses were formulated in the form of sum of squared differ-

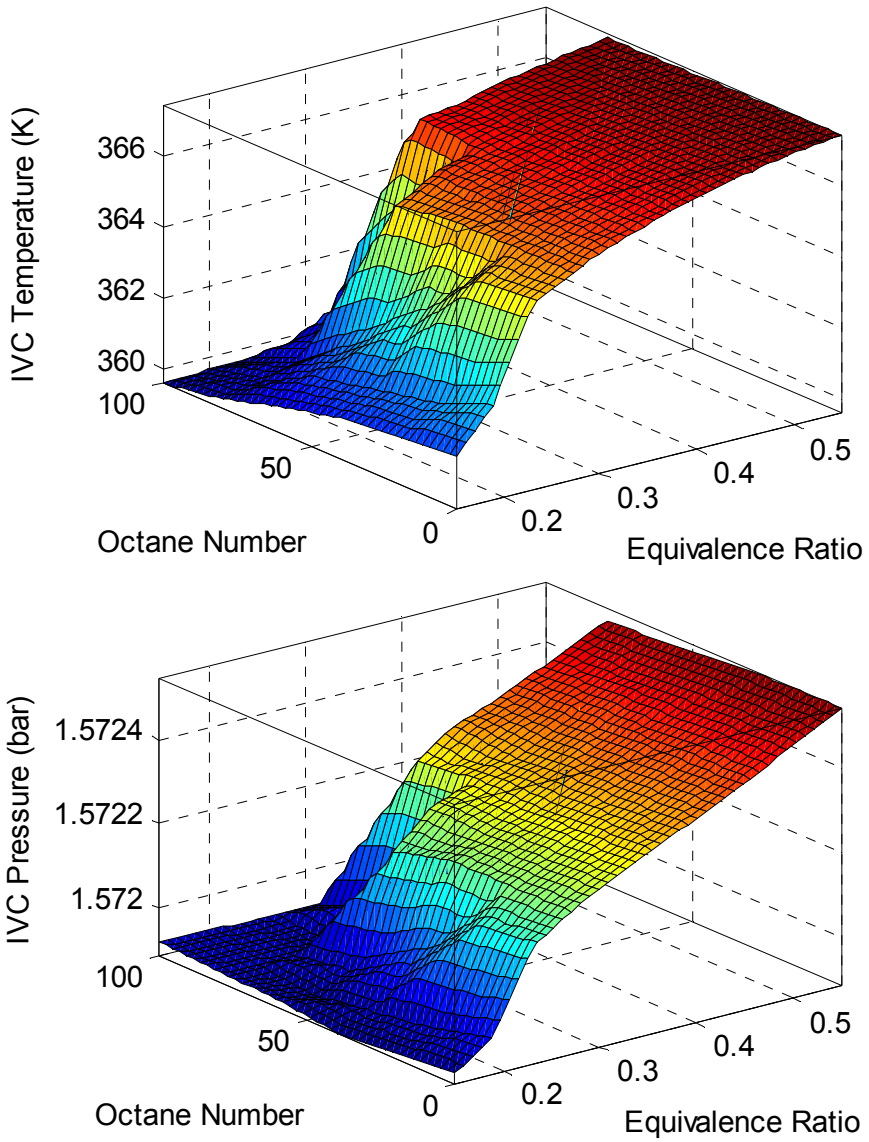

Figure 5: *IVC temperature and pressure maps for the engine speed of 1200 rpm. The maps (including those for other speeds) indicate that both equivalence ratio and speed had a moderate effect on IVC temperature, but a weak effect on IVC pressure. PRF ratio had little or no effect on IVC pressure and temperature.*

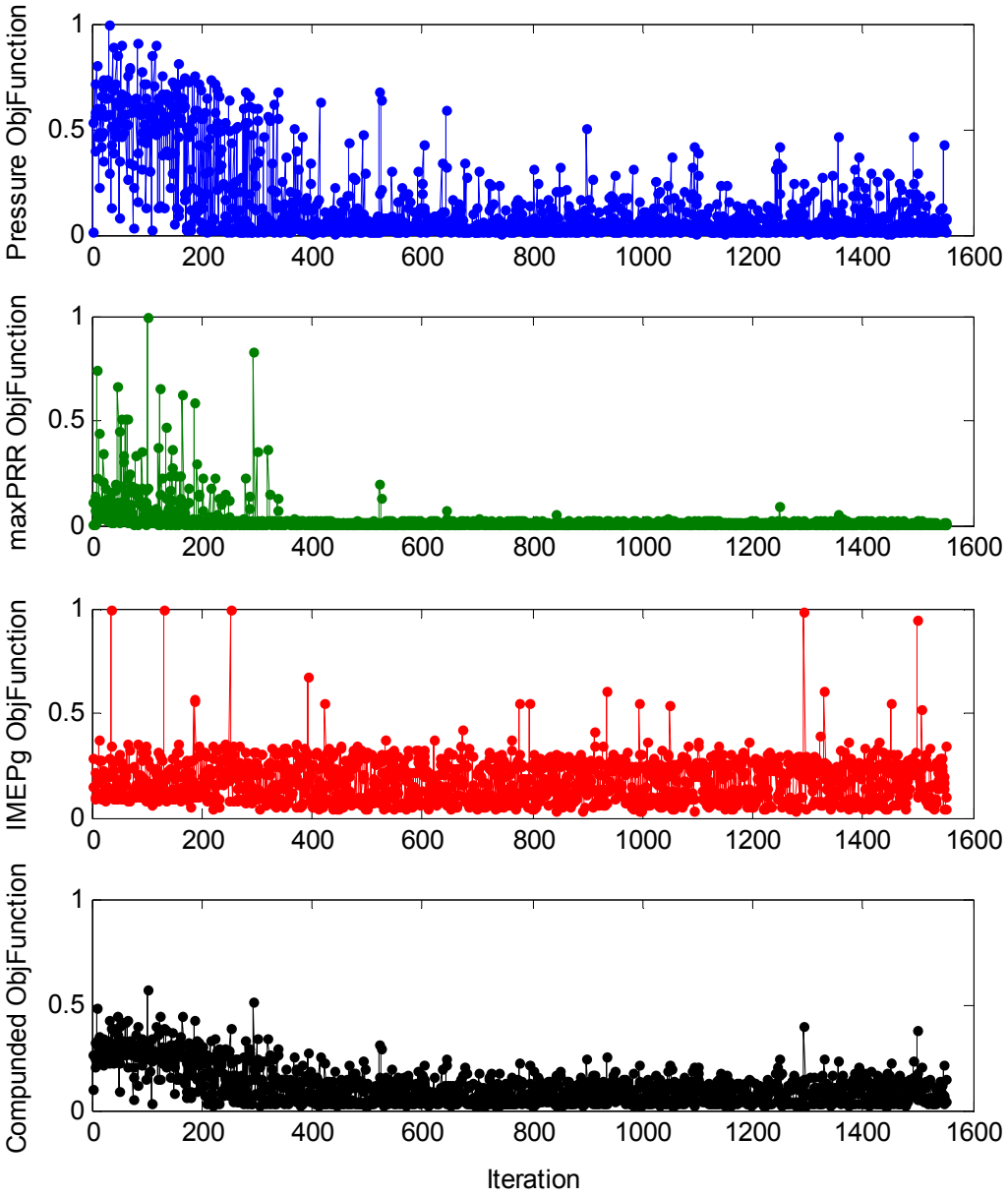

Figure 6: *History of objective function values throughout the multi-objective optimization run. A termination criterion was set based on settling of compounded objective function. The results show a low sensitivity of maximum pressure rise rate to changes in the optimization variables.*

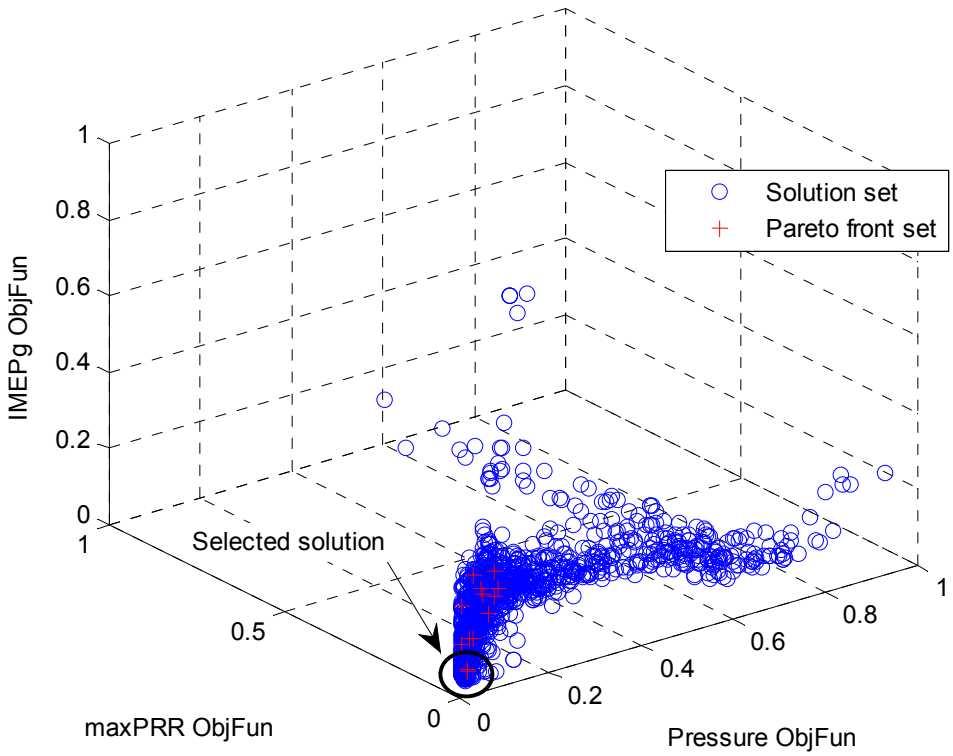

Figure 7: *Solution space with Pareto front set of optimum solutions. All Pareto solutions gave almost the same value for maximum pressure rise rate objective. As such, a Pareto front solution that gives the best compromise between cylinder pressure history and gross indicated work was selected.*

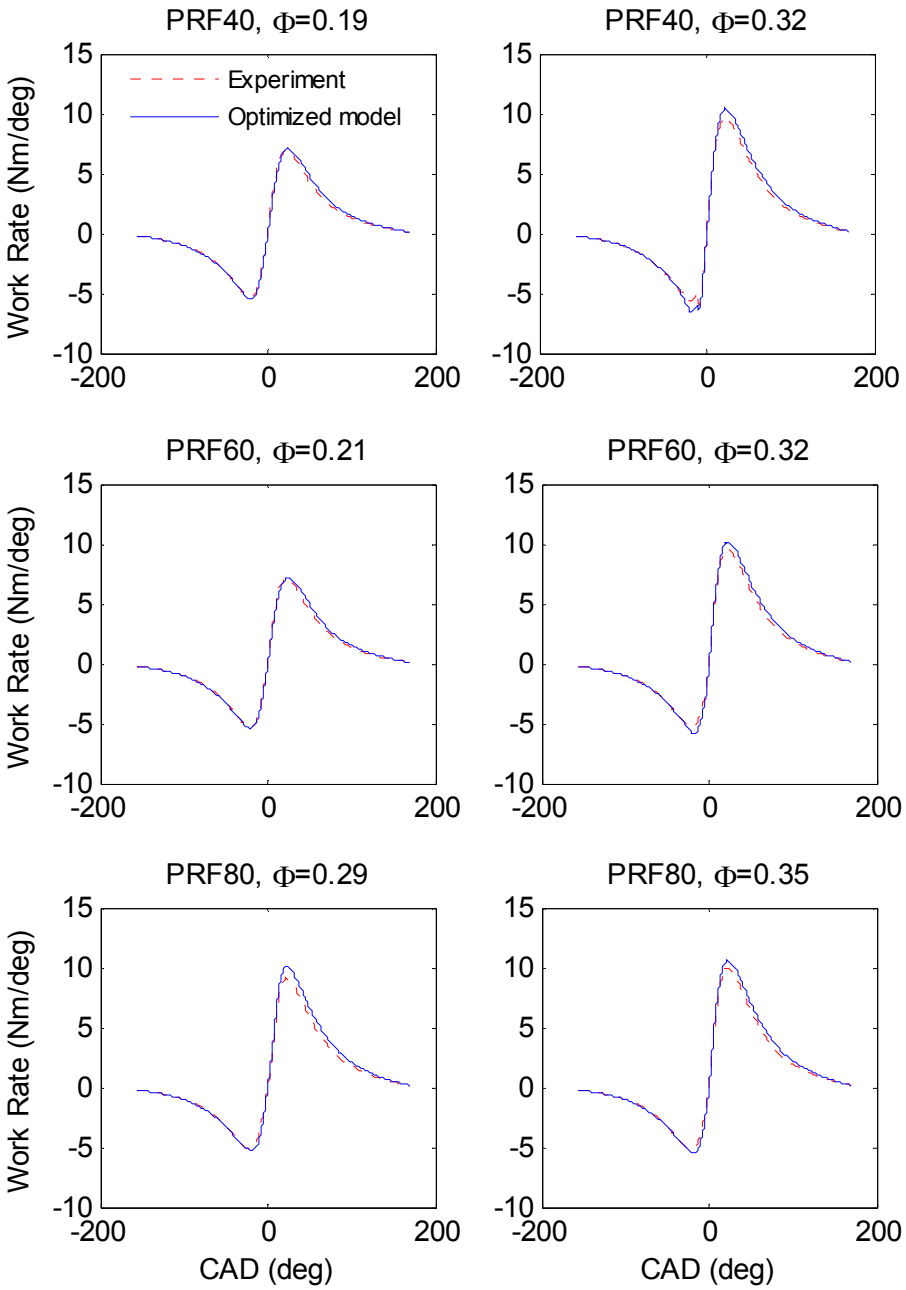

Figure 8: *Comparing model predicted work rate with experimental data at 1200 rpm. A very good fit can be seen across the tested engine operating window. However, there is a slight, but consistent, over prediction of pressure value during the expansion process. The accumulation of this error leads to a significant, but fairly consistent, deviation in predicted IMEPg values.*

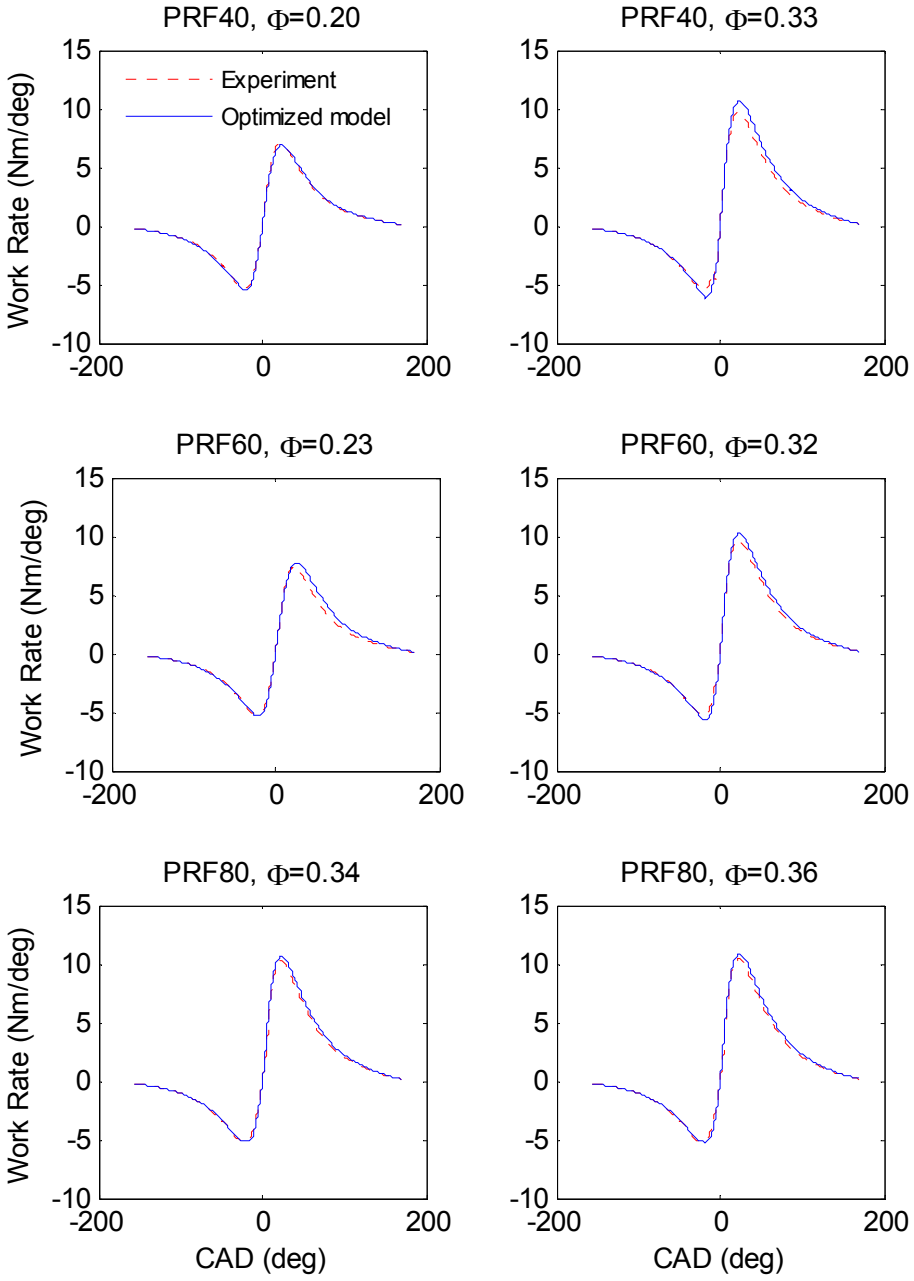

Figure 9: *Comparing model predicted work rate with experimental data at 1500 rpm. As in the case of 1200 rpm, the fit with experiments is good despite the consistent over prediction of pressure value during the expansion process.*

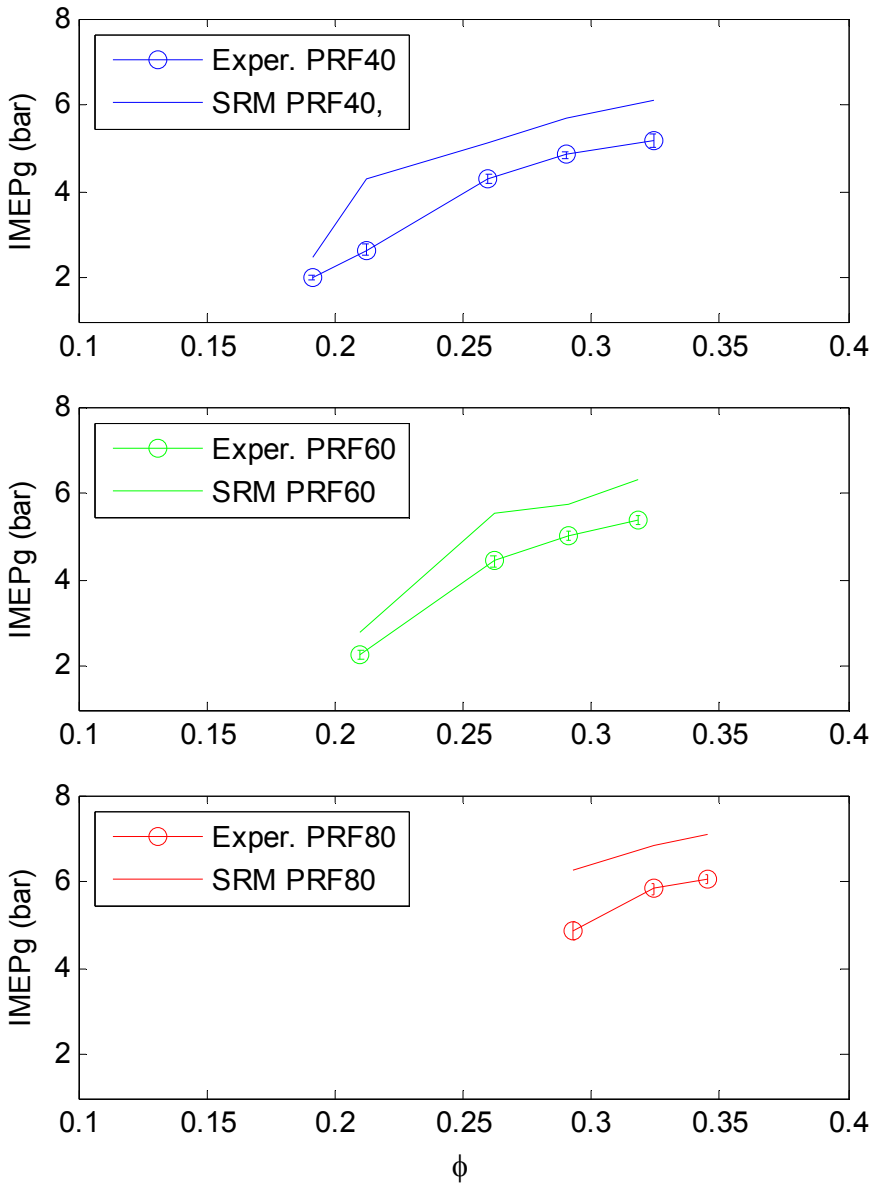

Figure 10: *Comparing model predicted gross IMEP with experimental data at 1200 rpm. The model consistently over predicts the gross work, with an estimated average error of about 20%. Error bars on experimental data are based on ± 1 standard deviation.*

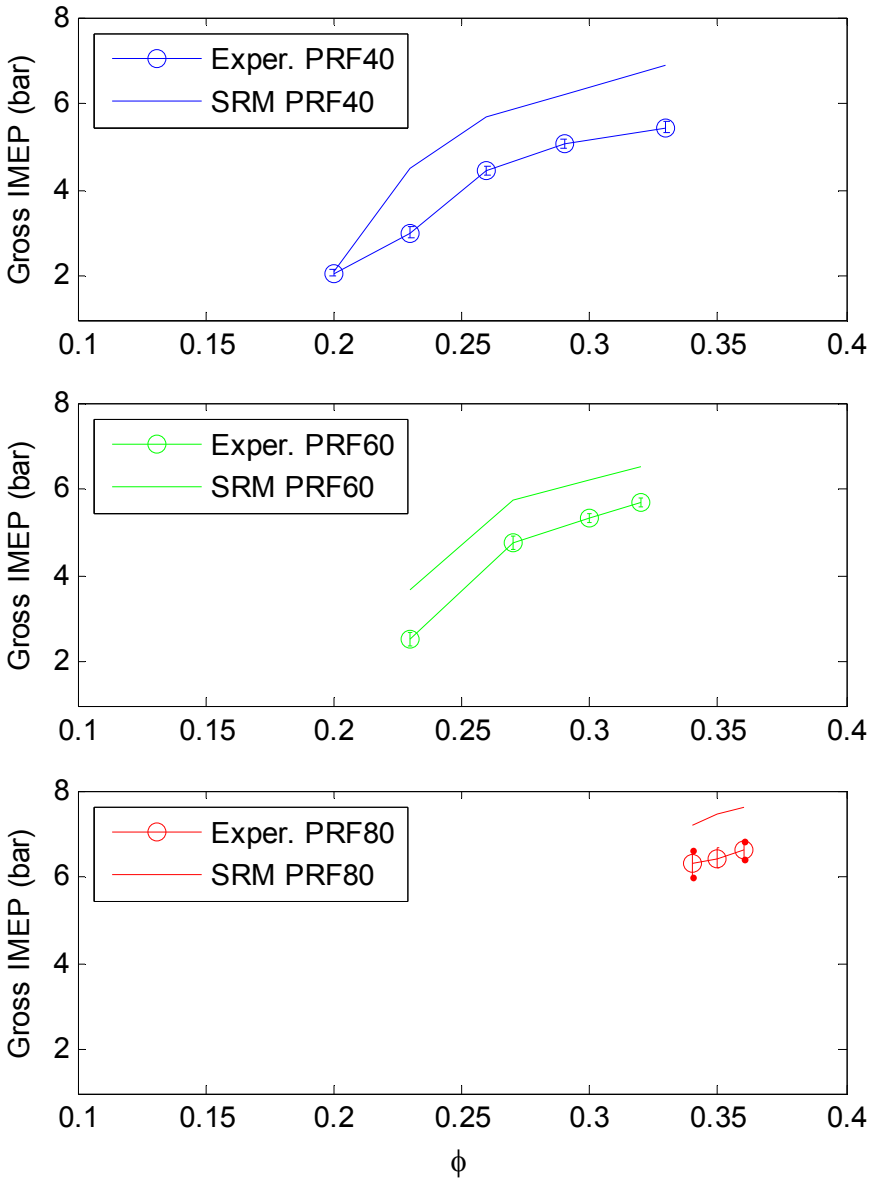

Figure 11: *Comparing model predicted gross IMEP with experimental data at 1500 rpm. Again, a consistent over prediction of gross work across the tested range is seen here. Error bars on experimental data are based on ±1 standard deviation.*

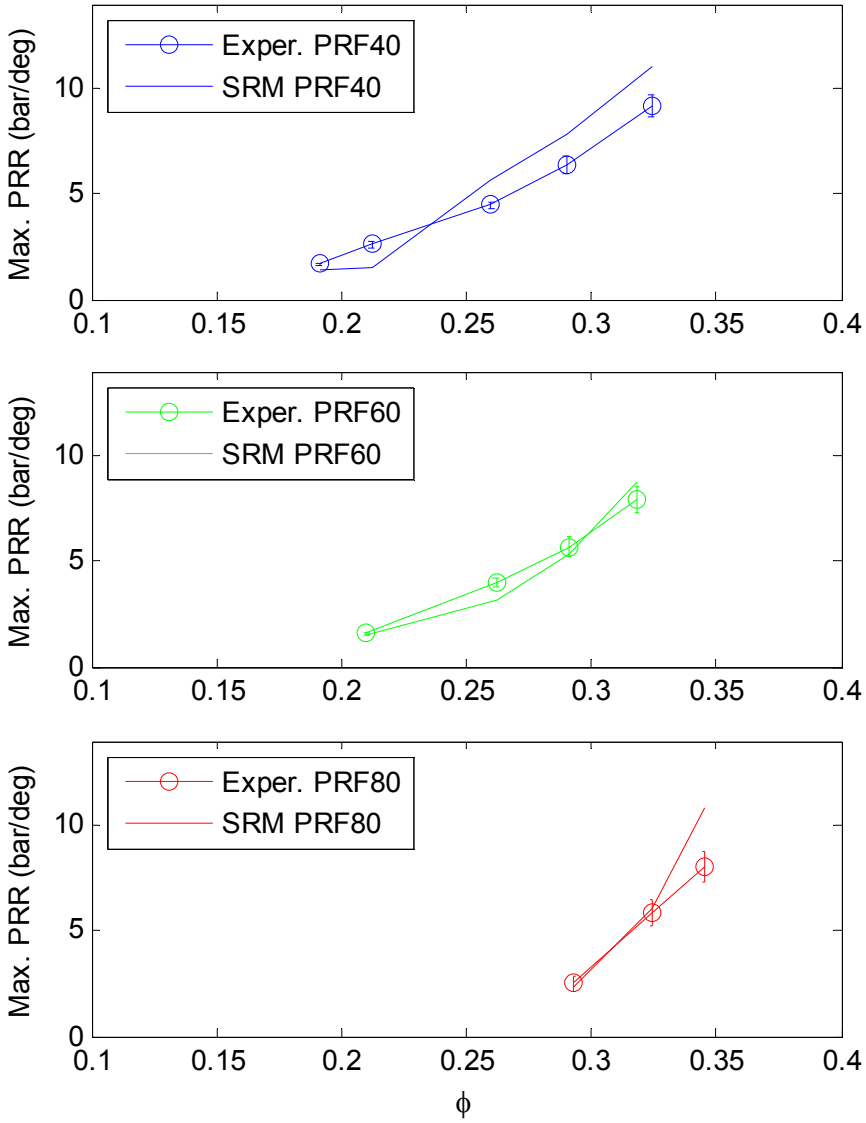

Figure 12: *Comparing model predicted maximum pressure rise rate with experimental data at 1200 rpm. Error bars on experimental data are based on ±1 standard deviation.*

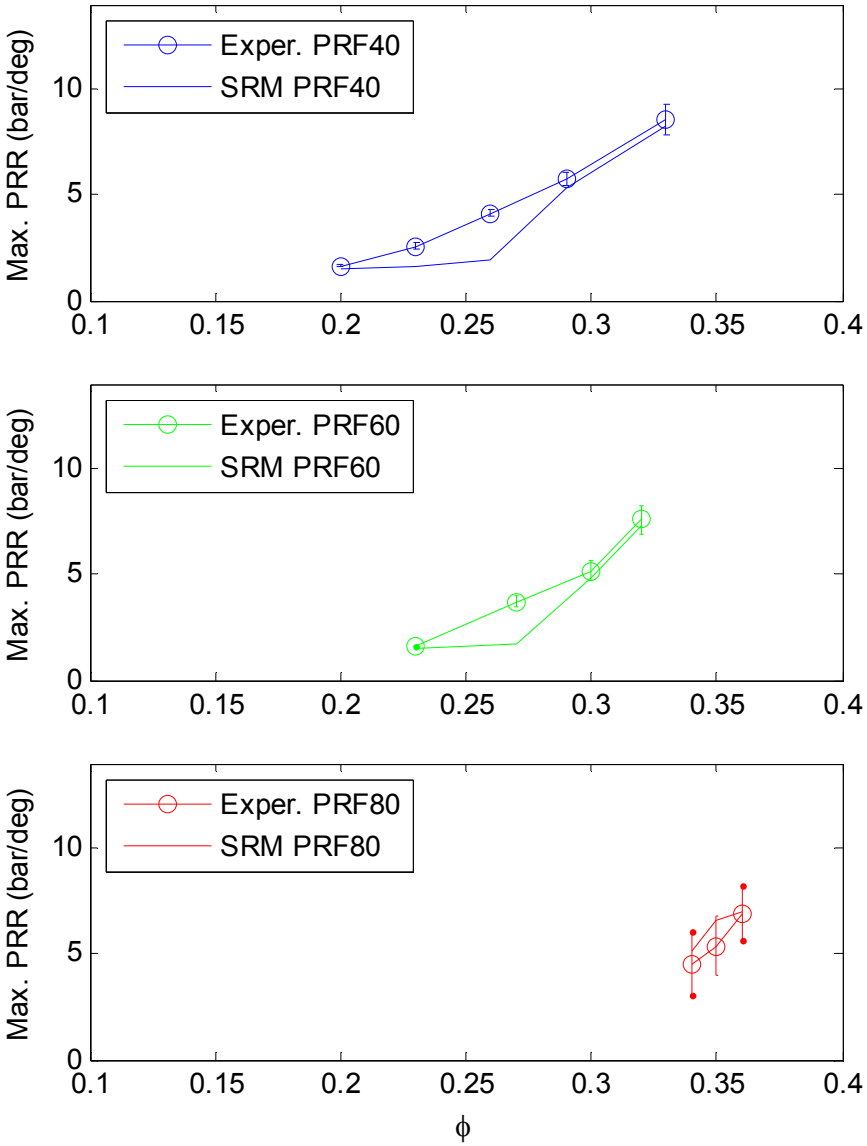

Figure 13: *Comparing model predicted maximum pressure rise rate with experimental data at 1500 rpm. Error bars on experimental data are based on ±1 standard deviation.*

ences between experiment and model values, and the optimization was carried out against results from 12 simultaneous experiments run at different operating conditions.

Optimization results are shown in Figures 6 and 7. Figure 6 shows the history of objective function values throughout the optimization run, which involved more than 1500 iterations (with each iteration taking about 10 minutes in average on a fairly fast machine). The optimization run was terminated after the compound objective function had fairly stabilized. The set of optimum solutions were then determined by constructing the Pareto front from the solution set, as shown in Figure 7. The selection of a particular solution from the Pareto set is down to the user and based on the weights he assigns to the different objectives. The results showed a low sensitivity of maximum pressure rise rate to changes in the optimization variables, and all Pareto solutions gave almost the same value for maximum pressure rise rate objective. As such, a Pareto front solution that gives the best compromise between cylinder pressure history and gross indicated work was selected.

To check the performance of the selected solution, several comparisons with experimental data for indicated work rate (which reflects cylinder pressure/volume changes), maximum pressure rise rate, and gross indicated work were made. These comparisons are shown in Figures 8-13. A very good fit can be seen across the tested engine operating window. There is a consistent over prediction of pressure value during the expansion process (as can be inferred from Figures 8 and 9), which in turn leads to consistently higher values of predicted gross indicated work (as can be seen in Figures 10 and 11). This resulting accumulated error in IMEPg is in the range of 20%. The specific causes of this over-prediction have not been examined in this work. However, the original mechanism (i.e. before optimization) exhibited significant over-prediction of pressure throughout the reactive part of the closed-volume cycle. Over-prediction during the expansion process persisted even after the optimization step. This could be simply an indication of a deficiency in the chemistry, but could also indicate that more emphasis should have been put on the expansion side when formulating the optimization objective function of cylinder pressure . The current function accounts for a total of five points on the pressure curve with only two on the expansion side (more discussion on how the objective functions were formulated can be found in [3]).

4 Results and Discussions

In order to assess the dual-fuel control approach in transient operating conditions and beyond the limits tested in the experiments, a dynamic control study was conducted using a simulation code that incorporates the optimized HCCI model (explained in the previous section) and allows for multi-cycle transient operation and closed-loop control of fuel ratio. This setup simulates a dual-fuel HCCI engine similar to that depicted in Figure 1, where the operation range is extended as possible by varying the ratio of the low-reactivity and high-reactivity fuels. Specifically, the fuels used here are the n-heptane (which has an octane number of 0) and the iso-octane (which has an octane number of 100). Varying the ratio between these two primary reference fuels affects the fuel reactivity and thus the heat release rate, which eventually affects the engine operability range.

An appropriate control strategy is needed to ensure that optimum fuel ratio is delivered

for each operation condition. A PID controller is typically used for this purpose (see [2, 5, 9, 10, 15]). Such controller, however, requires prior knowledge about the system responses and the optimum target values of controlled quantities. Also, the non-linearity of system responses (which exist in the engine case) will normally require careful tuning of the controller and non-trivial gain scheduling. This has been avoided in the current study by using a search algorithm that looks for a fuel ratio that maximizes the gross indicated work. Such control strategy, as the results suggest, appears to be sufficient to control pressure rise rate and combustion phasing while not needing any prior knowledge or preset information about them. It also ensures that the engine is always delivering maximum work at each operating condition. This is in a sense analogous to the use of maximum brake torque timing in spark-ignition engines.

The search for optimum PRF ratio is carried out in the current model using MATLAB's "fminbnd" algorithm, which is based on golden section search and parabolic interpolation [1]. This algorithm proved to be efficient as it normally took only 2-6 cycles to locate the optimum PRF ratio. However, because the algorithm works by cornering the solution within increasingly smaller intervals, large spikes in engine operation are expected during the initial intervals (as can be seen in the current results). Although different search algorithms may perform differently, the need for real time search could potentially make the approach very difficult to implement on a real engine.

Figures 14-17 show the results for running the model at engine speeds of 1200, 1500, and 1800 rpm. In all cases, the model simulates an HCCI engine subjected to an equivalence ratio sweep and where the controller at each condition seeks to maximize the gross indicated work (IMEPg) by varying the iso-octane between 0 and 100% in a mixture of iso-octane and n-heptane. Each equivalence ratio step lasts for 20 full cycles, during which the controller should have located the optimum PRF ratio and operation has stabilized.

Figure 14 demonstrates how the used control strategy ensures delivery of maximum work at each operation condition. The case where a controller is used is compared to three fixed PRF ratio fuels (PRF20, PRF50, and PRF80). The controlled case was consistently able to deliver maximum work at all conditions. The performance of other fuels varied across the sweep, and in most cases the delivered work was by far lower than the controlled case.

The benefit of dual-fuel control approach on HCCI operation range is demonstrated in Figure 15. Here, the simulation results at 1200 rpm show how using a fixed PRF ratio fuel adversely limits the operating range of this HCCI engine. The operating limits are set based on maximum pressure rise rate, where the upper limit (i.e. the knocking limit) is at about 10 bar/deg and the lower limit (i.e. the misfire limit) is about 2 bar/deg (this agrees well with the experimental data presented in Figure 3 where 5% IMEP CoV corresponds to about 2 bar/deg). While fixed PRF ratio fuels resulted in significantly limited operating ranges, varying the PRF octane rating between 0-100 kept the HCCI combustion within the set limits almost over the whole sweep. It can also be seen that, without any prior knowledge about optimum combustion phasing, the employed control strategy kept the CA50 under control almost over the whole sweep.

Similar results have been obtained for the engine speeds of 1500 and 1800 rpm. These results are shown respectively in Figures 16 and 17. By combining the results for the different speeds, a map of optimum PRF ratio for the different speeds and equivalence

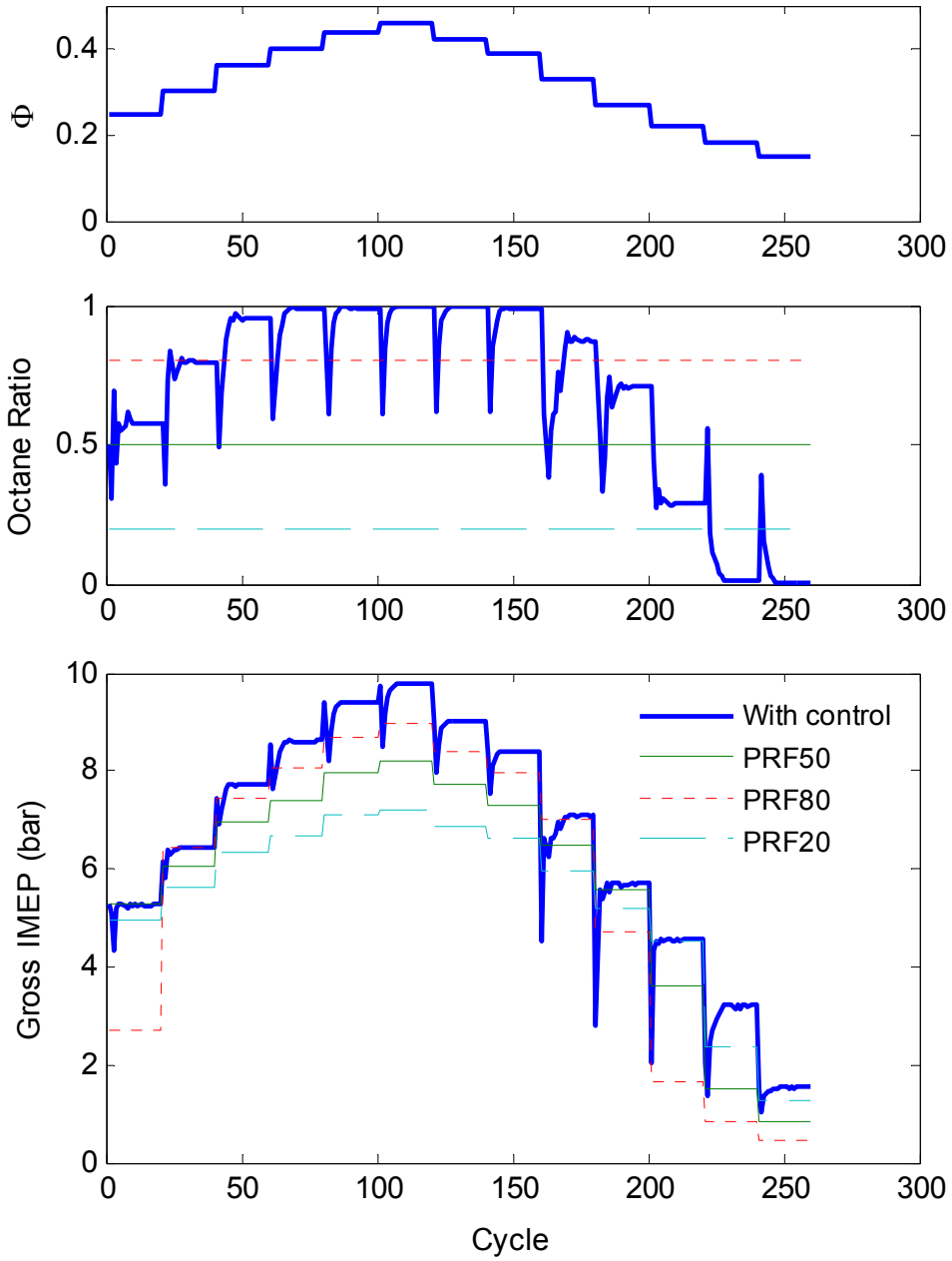

Figure 14: *Dynamic simulation of octane ratio control to maintain maximum work at 1200 rpm. Here, the controlled case is compared to three fixed PRF ratio fuels (PRF20, PRF50, and PRF80). The controlled case was consistently able to deliver maximum work at all conditions. Performance of other fuels varied across the sweep, and in most cases the delivered work was noticeably lower than the controlled case.*

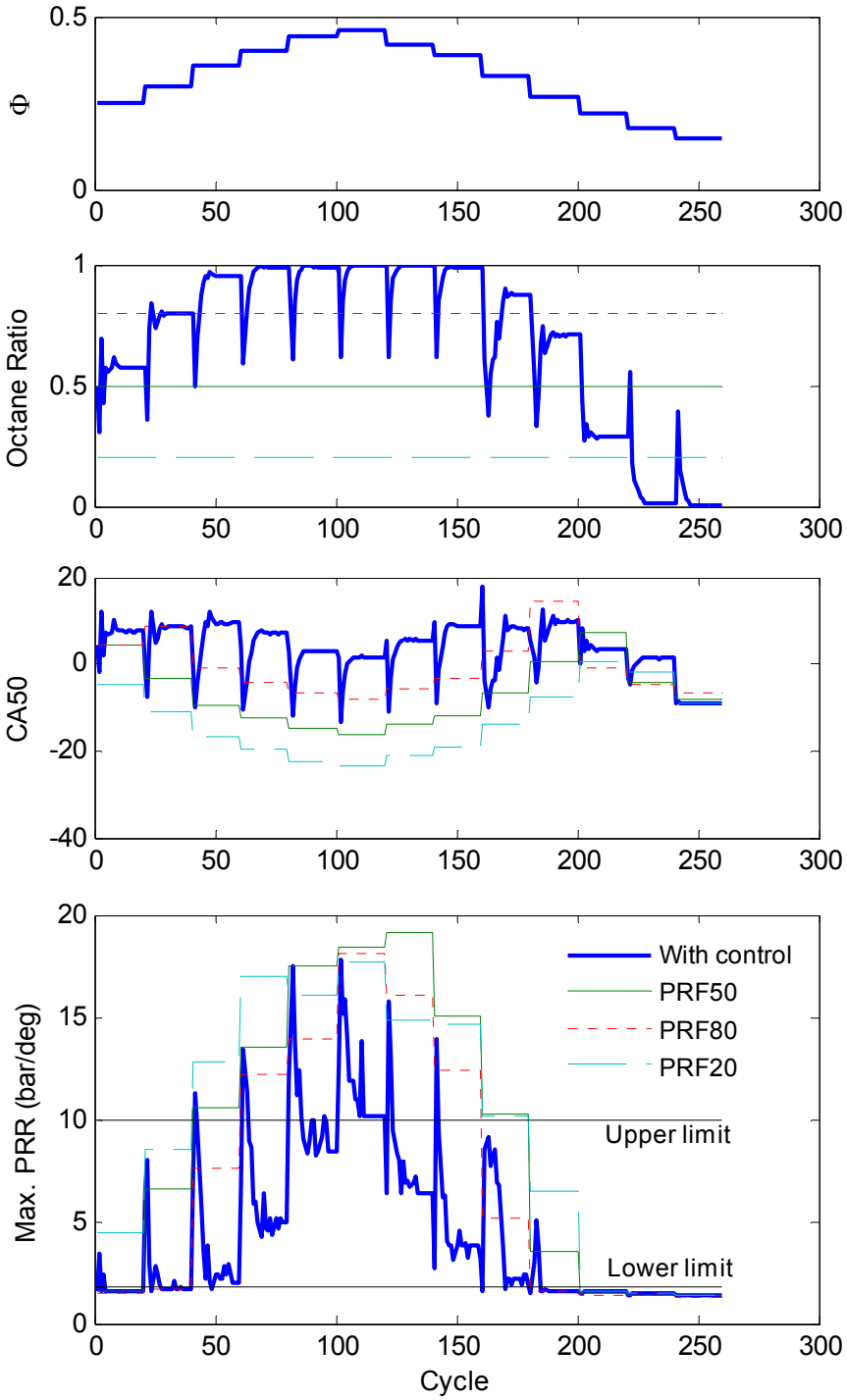

Figure 15: *Effects of octane ratio control on CA50 and maximum pressure rise rate at 1200 rpm. While fixed PRF ratio fuels resulted in significantly limited operating ranges, varying the PRF octane rating between 0-100 kept the HCCI combustion within the set limits almost over the whole sweep.*

ratios can be constructed. This map, shown in Figure 18, can now replace the controller for further investigations within the operating ranges and conditions considered in this study.

The HCCI operating envelope as predicted by the model with PRF ratio control and work maximization objective is compared to those operating envelopes obtained from experiments with fixed PRF octane rating of 40, 60, and 80. This comparison is shown in Figure 19. These envelopes, as mentioned before, represent the possible operating windows between misfire and knocking limits. It should be noted that the lower part of the figure represents the maximum gross work when optimum PRF ratio is used at each equivalence ratio. The size of the operating envelope is therefore better represented by the equivalence ratio map on the upper part of the figure.

In terms of equivalence ratio and gross indicated work (IMEPg), the predicted expansion in the operating windows was significant especially with respect to the upper operating limit. For example, increasing the octane rating from 80 to 100 at 1200 rpm allowed for an increase in the equivalence ratio range from 0.34 to 0.42. This in turn increased the gross indicated work by about 50% (that is with the consideration of the error in the model prediction of gross indicated work). In general, the results indicate that the dual-fuel approach, using iso-octane and n-heptane, could potentially allow an HCCI load range equivalent to about 60% of a typical boosted spark-ignition engine. However, as the study only considered a narrow speed range, more work is needed to examine this potential at higher speeds.

5 Summary and Conclusions

A dual-fuel approach using primary reference fuels to control combustion in HCCI engine is investigated in this work both experimentally and through a simulation study. Experiments were performed on a single-cylinder research engine fueled with different ratios of primary reference fuels and operated at different speed and load conditions.

The results from these experiments showed a clear potential for the dual-fuel approach to extend the HCCI engine operating window. Engine operation envelopes constructed from the results showed a significant effect of PRF octane rating on HCCI operation. While the envelopes shrink as the PRF octane rating increases, they also allow the engine to operate at higher equivalence ratios and to produce more work. These effects generally become more prominent as the speed increases. The results also showed a clear advantage of selecting an optimum PRF ratio on the engine positive work for each operating condition.

In order to assess the dual-fuel control approach in transient operating conditions and beyond the limits tested in the experiments, a dynamic control study was conducted using a simulation code that incorporates a stochastic reactor HCCI model and allows for multi-cycle transient operation and closed-loop control of fuel ratio.

The HCCI model utilizes a highly reduced PRF mechanism that has only 33 species and 38 reactions. This limited chemistry representation along with the other simplifications (such as using a fixed EGR ratio and composition) necessitated an optimization step to enhance the model predictivity of those responses relevant to the current study. The model

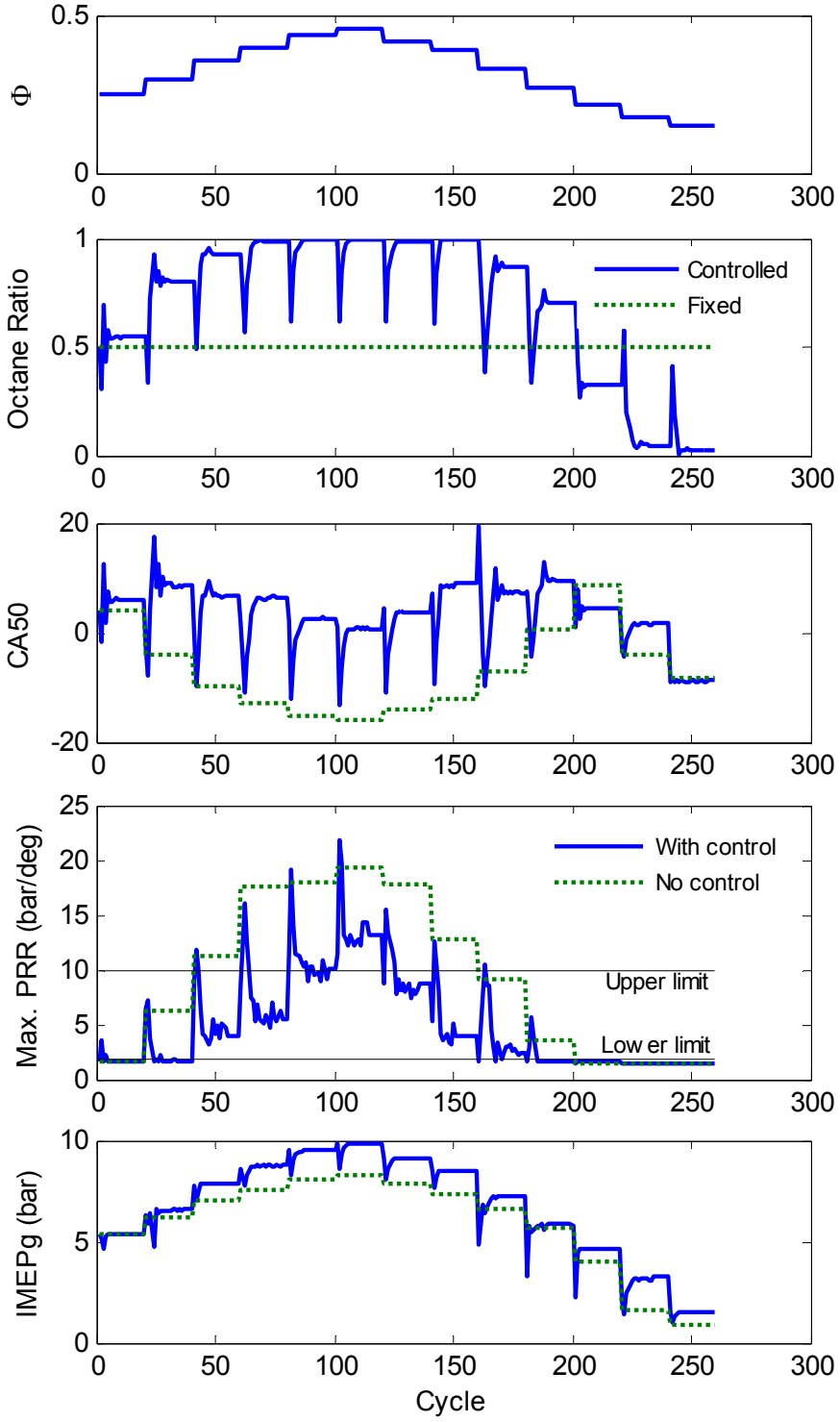

Figure 16: *Dynamic simulation of octane ratio control to maintain maximum work at 1500 rpm.*

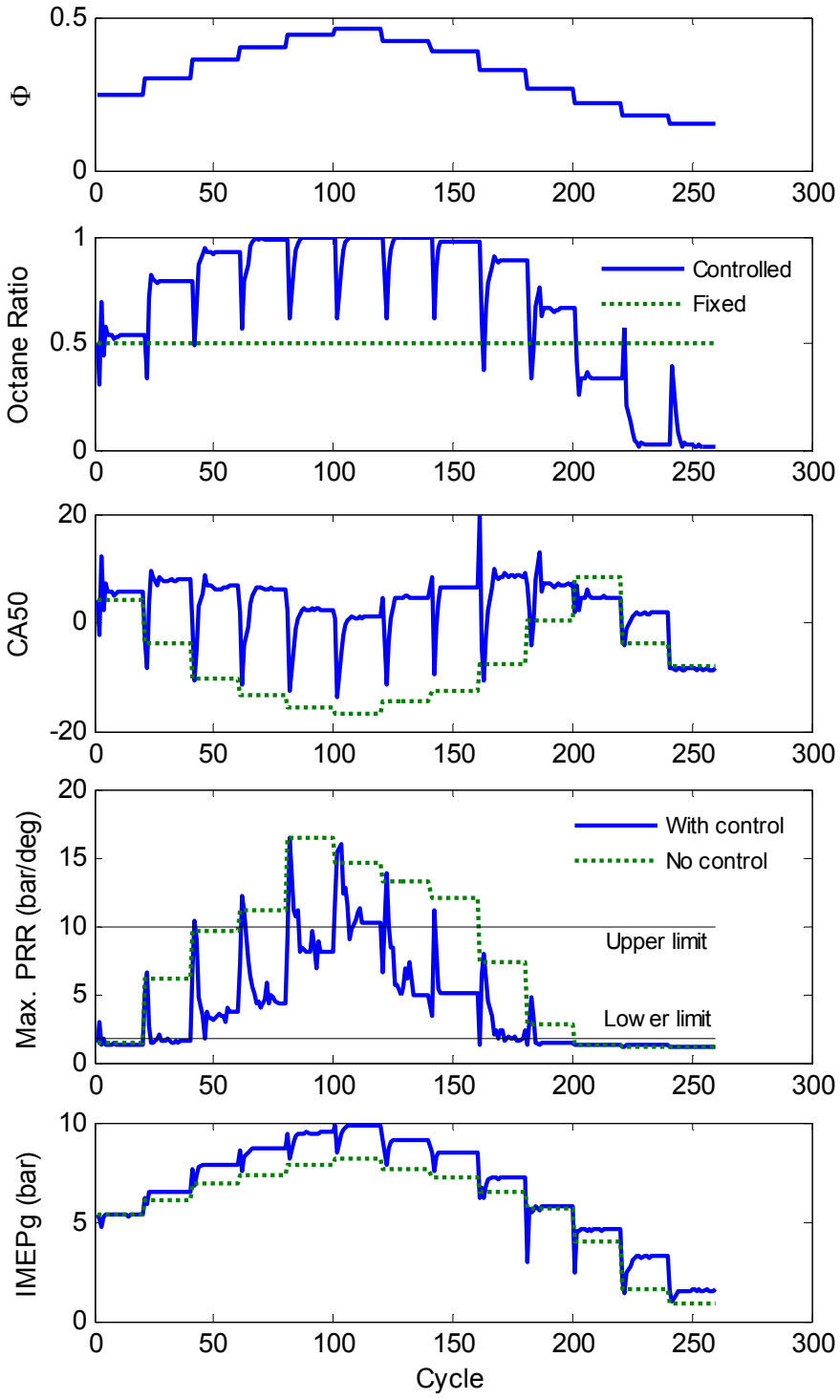

Figure 17: *Dynamic simulation of octane ratio control to maintain maximum work at 1800 rpm.*

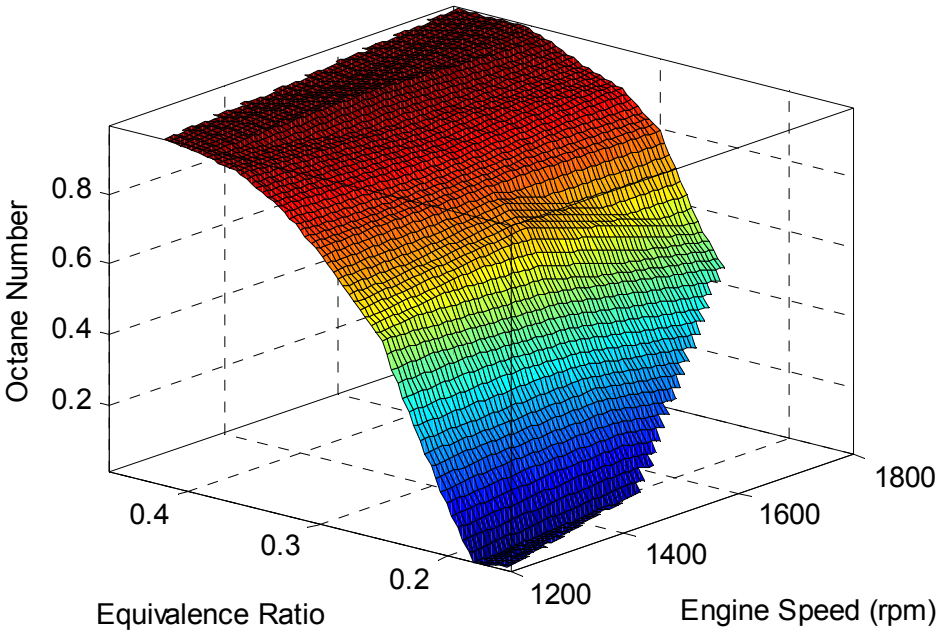

Figure 18: *Optimum PRF octane rating map for different engine speeds and equivalence ratios.*

was optimized using a multi-objective genetic algorithm, where the best solutions are searched for using the principles of evolution. To check the performance of the optimized model, several comparisons with experimental data for indicated work rate, maximum pressure rise rate, and gross indicated work were made.. Except for the gross indicated work where a large but consistent error persisted, a good fit with the experiment was seen across a wide range of operating conditions.

The closed-loop control of fuel ratio employed in this study is based on a search algorithm, where the objective is to maximize the gross work rather than directly controlling the combustion phasing to match preset values. The use of this search algorithm, while providing an efficient performance, allowed for avoiding the difficulties associated with tuning a PID controller. It also proved effective in controlling pressure rise rate and combustion phasing (measured by CA50) while not needing any prior knowledge or preset information about them. Above all, this control strategy ensured that the engine is always delivering maximum work at each operating condition. However, the need for real-time search could potentially make this approach very difficult to implement on a real engine.

While fixed PRF ratio fuels resulted in significantly limited operating ranges, varying the PRF octane rating between 0-100 kept the HCCI combustion within the set limits over a wide equivalence ratio range. Results from the dynamic control model allowed for mapping the optimum PRF ratio for the different speeds and equivalence ratios, and for constructing a full operating envelope for a dual-fuel case where PRF octane rating is varied from 0 to 100. Comparing this model-predicted envelope to those obtained from the experiments provided a useful insight on the potential of the duel-fuel approach as a means for controlling HCCI combustion and extending its operating range.

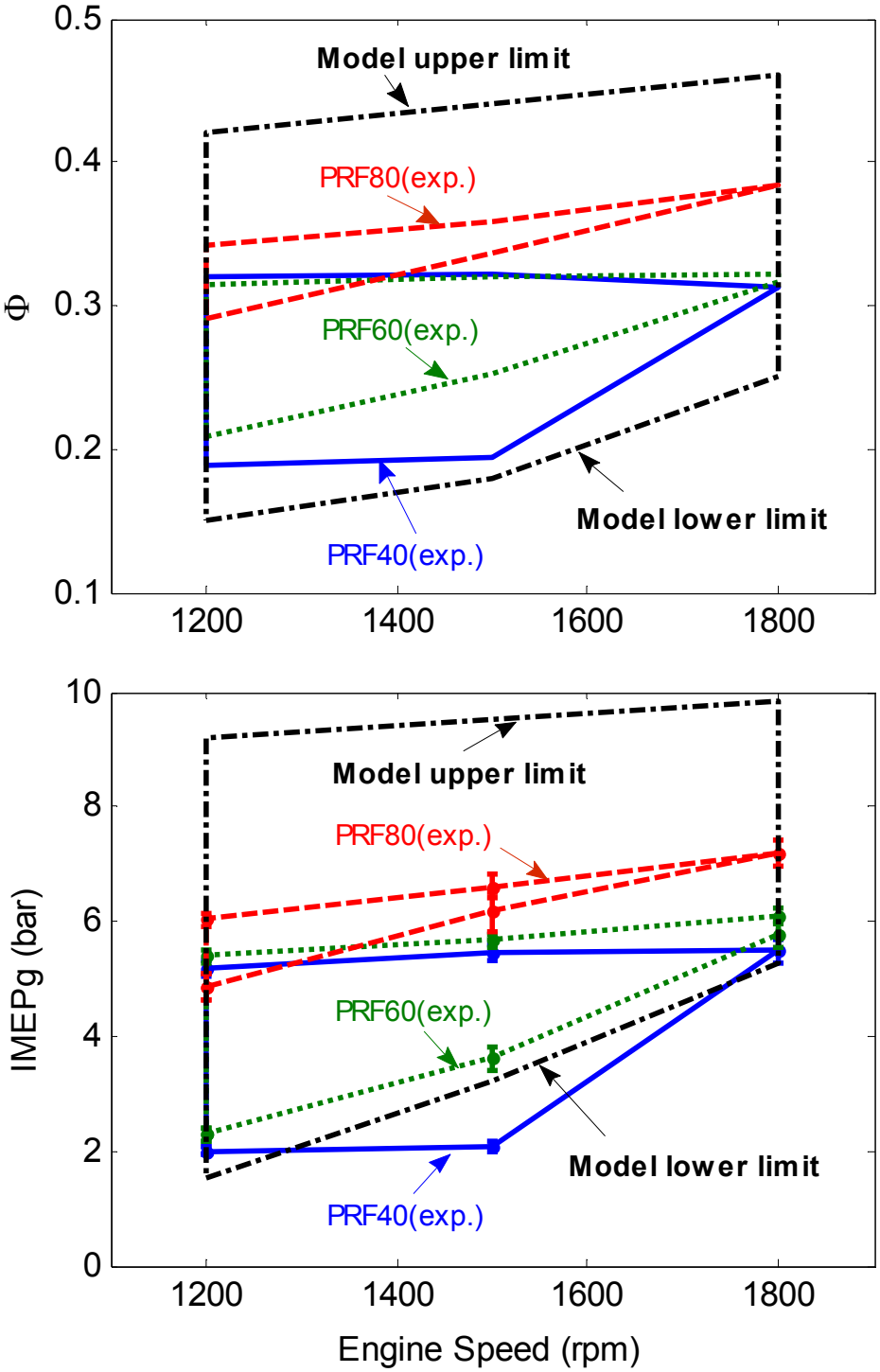

Figure 19: *Expansion of HCCI engine operating envelope by varying the PRF octane rating from 0 to 100. The resulting envelope is compared to those obtained from engine experiments run with three constant PRF ratios. Predicted expansion in the operating windows is significant especially with respect to the upper operating limit.*

In general, the results indicated that the dual-fuel approach, using iso-octane and n-heptane, could potentially enable an HCCI load range equivalent to about 60% of a typical boosted spark-ignition engine. However, as the study only considered a narrow speed range, more work is needed to examine this potential at higher speeds. It is also important to note that, while the use of primary reference fuels is convenient to generally represent gasoline-like fuels, the performance of actual gasoline or gasoline-like fuels could be immensely different in HCCI engine. While the current study tries to provide a useful insight on the potential of the dual-fuel approach, the fuel effects will certainly need to be taken into account when quantifying this potential.

6 Acknowledgement

The authors would like to thank Yoann Viollet, Marcin Plociniczak and Hassan Babiker of Saudi Aramco's R&D Center for their help in carrying out the HCCI engine experiments.

7 Definitions, Acronyms and Abbreviations

ATDC	After top dead centre
BTDC	Before top dead centre
CAD	Crank angle degree
CoV	Coefficient of variation
EVC	Exhaust valve closure
EVO	Exhaust valve opening
HCCI	Homogeneous charge compression ignition
IMEPg	Gross indicated mean effective pressure
IVC	Intake valve closure
IVO	Intake valve opening
PFI	Port fuel injection
PID	Proportional, integral, and differential
PRF	Primary reference fuel
SRM	Stochastic reactor model
TDC	Top dead centre
Φ	Equivalence ratio

References

[1] MATLAB 7 User Guide. The MathWorks Inc., 2009.

[2] A. Aldawood, S. Mosbach, and M. Kraft. HCCI combustion phasing transient control by hydrogen-rich gas: Investigation using a fast detailed-chemistry full-cycle model. *SAE Paper No. 2009-01-1134*, 2009.

[3] A. Aldawood, S. Mosbach, M. Kraft, and A. Amer. Multi-objective optimization of a kinetics-based hcci model using engine data. *SAE Paper No. 2011-01-1783*, 2011.

[4] M. Atkins and C. Koch. The effect of fuel octane and dilutent on homogeneous charge compression ignition combustion. *Proceedings of the Institution of Mechanical Engineers, Part D: Journal of Automobile Engineering*, 219, 2005.

[5] J. Bengtsson, P. Strandh, R. Johansson, P. Tunestl, and B. Johansson. Closed-loop combustion control of homogeneous charge compression ignition (hcci) engine dynamics. *International Journal of Adaptive Control and Signal Processing*, 2004.

[6] A. Bhave, M. Kraft, L. Montorsi, and F. Mauss. Modelling a dual-fuelled multi-cylinder HCCI engine using a PDF based engine cycle simulator. *SAE Paper No. 2004-01-0561*, 2004.

[7] A. Bhave, M. Kraft, F. Mauss, A. Oakley, and H. Zhao. Evaluating the EGR-AFR operating range of a HCCI engine. *SAE Paper No. 2005-01-0161*, 2005.

[8] J. Cha, S. Kwon, and S. Park. An experimental and modelling study of the combustion and emission characteristics for gasoline-diesel dual-fuel engines. *Proceedings of the Institution of Mechanical Engineers, Part D: Journal of Automobile Engineering*, 225, 2011.

[9] P. T. G. Haraldsson and B. Johansson. Hcci combustion phasing with closed-loop combustion control using variable compression ratio. *SAE Technical Paper 2003-01-1830*, 2003.

[10] G. Haraldsson, P. Tunestl, and B. Johansson. Hcci closed-loop combustion control using fast thermal management in a multi cylinder engine. *SAE Technical Paper 2004-01-0943*, 2004.

[11] S. Kokjohn, R. Hanson, D. Splitter, and R. Reitz. Experiments and modeling of dual-fuel hcci and pcci combustion using in-cylinder fuel blending. *SAE Technical Paper 2009-01-2647*, 2009.

[12] X. Lu, W. Chen, Y. Hou, , and Z. Huang. Study on the ignition, combustion and emissions of hcci combustion engines fuelled with primary reference fuel. *SAE Paper No. 2005-01-0155*, 2005.

[13] J. Ma, X. L, L. Ji, and Z. Huang. An experimental study of hcci-di combustion and emissions in a diesel engine with dual fuel. *International Journal of Thermal Sciences*, 47, 2008.

[14] S. Mosbach, M. Kraft, A. B. F. Mauss, J. Mack, and R. Dibble. Simulating a homogenous charge compression ignition engine fuelled with a DEE/EtOH blend. *SAE Paper No. 2006-01-1362*, 2006.

[15] J. Olsson, P. Tunestl, and B. Johansson. Closed-loop control of an hcci engine. *SAE Paper No. 2001-01-1031*, 2001.

[16] Tanaka, F. Ayala, J. Keck, and J. Heywood. Two-stage ignition in hcci combustion and hcci control by fuels and additives. *Combustion and Flame*, 132, 2003.

[17] T. Tsurushima. A new skeletal prf kinetic model for hcci combustion. *Proceedings of the Combustion Institute*, 2009.

[18] L. Xingcai, H. Yuchun, Z. Linlin, and H. Zhen. Experimental study on the auto-ignition and combustion characteristics in the homogeneous charge compression ignition (hcci) combustion operation with ethanol/n-heptane blend fuels by port injection. *Fuel*, 85, 2006.